UNIVERSITY OF LEEDS

This is a repository copy of *HIFU Power Monitoring Using Combined Instantaneous Current and Voltage Measurement*.

White Rose Research Online URL for this paper:
http://eprints.whiterose.ac.uk/152553/

Version: Accepted Version

Article:
Adams, C, McLaughlan, JR orcid.org/0000-0001-5795-4372, Carpenter, TM orcid.org/0000-0001-5676-1739 et al. (1 more author) (2020) HIFU Power Monitoring Using Combined Instantaneous Current and Voltage Measurement. IEEE Transactions on Ultrasonics, Ferroelectrics, and Frequency Control, 67 (2). ISSN 0885-3010

https://doi.org/10.1109/TUFFC.2019.2941185

© 2019 IEEE. This is an author produced version of a paper published in IEEE Transactions on Ultrasonics, Ferroelectrics, and Frequency Control. Personal use of this material is permitted. Permission from IEEE must be obtained for all other uses, in any current or future media, including reprinting/republishing this material for advertising or promotional purposes, creating new collective works, for resale or redistribution to servers or lists, or reuse of any copyrighted component of this work in other works. Uploaded in accordance with the publisher's self-archiving policy.

Reuse
Items deposited in White Rose Research Online are protected by copyright, with all rights reserved unless indicated otherwise. They may be downloaded and/or printed for private study, or other acts as permitted by national copyright laws. The publisher or other rights holders may allow further reproduction and re-use of the full text version. This is indicated by the licence information on the White Rose Research Online record for the item.

Takedown
If you consider content in White Rose Research Online to be in breach of UK law, please notify us by emailing eprints@whiterose.ac.uk including the URL of the record and the reason for the withdrawal request.

White Rose university consortium
Universities of Leeds, Sheffield & York

eprints@whiterose.ac.uk
https://eprints.whiterose.ac.uk/

HIFU Power Monitoring Using Combined Instantaneous Current and Voltage Measurement

Chris Adams, James R. McLaughlan, Thomas M. Carpenter, and Steven Freear

***Abstract*—During HIFU therapy it is important that the electrical power delivered to the transducer is monitored to avoid under or over exposure, ensure patient safety and to protect the transducer itself. Due to ease of measurement, the transducer's potential difference may be as an indicator of power delivery. However, even when a transducer's complex impedance is well characterised at small amplitudes and matching networks are used, voltage-only (VO) monitoring cannot account for the presence of drive waveform distortion, changes to the acoustic path or damage to the transducer. In this study, combined current and voltage (CCV) is proposed as an MRI-compatible, miniature alternative to bi-directional power couplers that is compatible with switched amplifiers. For CCV power measurement, current probe data was multiplied by the voltage waveform and integrated in the frequency domain. Transducer efficiency was taken into account to predict acoustic power. The technique was validated with a radiation force balance (RFB). When using a typical HIFU transducer and amplifier, VO predictions and acoustic power had a maximum difference of 20%. However, under the same conditions, CCV only had a maximum difference of 5%. The technique was applied to several lesioning experiments and it was shown that when VO was used as a control between two amplifiers there was up to a 38% difference in lesion area. This greatly reduced to a maximum of 5% once CCV was used instead. These results demonstrate that CCV can accurately predict real-time electrical power delivery leading to safer HIFU treatments.**

I. Introduction

HIGH intensity focused ultrasound (HIFU) is a surgical technique that is used to generate necrosis in tissue via thermal [1], [2] or other mechanical effects such as cavitation [3], [4] or boiling [5]–[7]. The technique is highly localised, and it can be used to non-invasivley treat an area while sparing surrounding tissue. The main application area of HIFU is the treatment of soft tissue tumours [8], [9] in liver [10], kidney [11], prostate [12], [13], breast [14] and in the brain [15]–[19].

Magnetic resonance imaging (MRI) is frequently used to guide HIFU to provide real-time temperature maps [20]. Many thousands of patients worldwide have benefited from the combination of these technologies for treatment of uterine fibroids and bone tumours [21].

This work was supported by the U.K. Engineering and Physical Sciences Research Council under grant EP/K029835/1, the National Institute for Heart, Lung and Blood (NHLBI) under grant 1 U01 HL121838-01, the Wellcome Trust under grant 105615/Z/14/Z and the Royal Society under grant RG170324.

Chris Adams is at the Sunnybrook Research Institute, Toronto, Canada (e-mail: christopher.adams@sri.utoronto.ca)

All of the other authors are with the School of Electronic and Electrical Engineering, University of Leeds, Leeds LS2 9JT, U.K. (e-mail: J.R.McLaughlan@leeds.ac.uk).

For ultrasound imaging systems, the focus of electronics research has largely been on improving computational power and element count [22]. However, for HIFU systems where the continuous power ratings must be significantly higher [23], the focus has been on reducing the cost, size and complexity [24], [25] whilst maintaining MRI compatibility [26], [27]. The exception is transcranial systems where the element count continues to increase due to improved steering capabilities [16], [28]–[30]

When making thermally-formed lesions using HIFU, the total acoustic power is arguably the most critical value as it dictates the spatial-peak pulse-average intensity (I_{SPPA}) and spatial-peak temporal-average (I_{SPTA}), which both correlate with lesion volume (the latter being a better metric of heating for low duty cycle exposures [31]). If excessive power is applied, the transducers could be damaged [23] or worse yet, the patient's tissue could be heated to potentially fatal temperatures. If underexposure occurs, the treatment may result in failure. Systems therefore must be calibrated so the acoustic power and thus intensity can be reliably controlled [24].

The international standards recommend calculating the spatial-peak pulse-averaged intensity from free-field measurements made using a hydrophone [32]. Damage thresholds and bandwidth limitations of regular hydrophones along with propagation nonlinearities [7] make measurement of these fields at clinically relevant intensities impossible. Therefore, for regular hydrophones, the recommendation is to take measurements under quasi-linear conditions and scale them with drive voltage to predict intensity values at higher powers [32]. Several authors have suggested using fibre optic hydrophones instead, which have much higher damage thresholds and can therefore be used to measure the subtle variances in intensity due to nonlinear propagation [33], [34]. Measurements using hydrophones must be performed at low duty cycles. For higher intensities and duty cycles, the radiation force balance (RFB) is the gold standard. It provides total acoustic power and spatial-average intensity if the beam dimensions are known [32]. However, both hydrophone and RFB measurement must be made in the free field before an exposure and can make no guarantees for patient safety during therapy. Therefore, a technique that can monitor power delivery during a HIFU exposure is highly desirable.

In this paper, the feasibility of using combined current and voltage (CCV) to measure effective power and thus predict acoustic power from the efficiency will be assessed.

II. Current Methodologies

When the drive frequency of a voltage source is DC (ie $f = 0$ Hz), Ohm's law may be used to calculate the current flowing from the source to a load ($I = V/R$) and total power dissipation in a load ($P = I^2R$). However, when the voltage source has a non zero frequency (AC), the resistance R of the load must instead be substituted with the complex impedance Z. It is also common place to use RMS rather than peak values for voltage, current and power, so that power (S) can be represented by

$$S = V^2/\|Z\| \tag{1}$$

If the impedance phase angle (ϑ) is low, then active power (P) can be considered to be approximately the same as apparent power:

$$S \approx P \text{ if } \vartheta < \epsilon \tag{2}$$

This may prove accurate enough for simple experiments and some studies [33].

To reduce the phase lead/lag, HIFU transducers are commonly connected to their driving circuit via a matching network of capacitors, inductors, and sometimes resistors [35]. By ensuring that the impedance matches the source as closely as possible, energy conversion in the transducer, at the cost of bandwidth, can be maximised [36]. However, the bulkiness of matching networks make them unsuitable for dense array applications (>1000 elements), so other techniques are explored to reduce the impedance of transmitting elements [37]. Arrays may also include purposely non-uniform elements where the impedance varies significantly across the array [38].

If the phase angle cannot be made trivially small ($\vartheta > \epsilon$), the complex rather than mangnitude of the impedance may be included in the calculation to extract the active, ie dissipated power in the load [39]. Although calculating dissipated power in this way may be suitable for simple loads at low frequencies ($<$ 1 KHz), HIFU transducers are high frequency ($\approx$ 1 MHz), complex electro-mechanical devices where impedance is greatly influenced by the acoustic path. The material properties of the propogation medium [40], the presence of acoustic reflectors (eg bone), cavitation [41] and saturation [23] are all known to influence impedance.

Switched circuits, which are highly desirable alternatives to linear amplifiers, due to their improved efficiency and reduced size [19], [42], conduce harmonic distortion. Even minor harmonics generated by these circuits, greatly influence the voltage signal due to the frequency-varying reactance of the source and load impedances. Matters are further complicated by the fact that voltage may be reflected from the load back to the source, and that both source and load impedances can vary significantly with frequency. For these reasons, even accurate impedance measurements and matching networks (if space even allows) do not predicate the use of voltage-only (VO) to predict acoustic power accurately. VO therefore is not an accurate way to predict acoustic power and the inadequacies of using impedance and VO to predict acoustic power are known [43].

One method of measuring effective power is to use bi-directional power couplers [24], [42], [44], which consist of transformers attached to transmission lines. These couplers produce two voltage signals proportional to the forward and reflected power. The Sonalleve MR-HIFU system (Philips Healthcare, Netherlands) uses this technique. Due to the varying impedance of the transducer and the pulsed-wave operation of HIFU it may be necessary to use additional equipment to extract the peak, average and frequency-varying power. Their use of ferrous materials and insertion losses make them suboptimal for use in MRI guided array applications. The physical size of these couplers make them an untenable solution for dense transcranial arrays. Couplers could be re-located away from the MRI machinery and transducers, but this induces errors as cable length may be responsible for as much as 50% of power usage [45] and if the transducers are not well matched, further errors may be introduced [42], [46].

Authors have already presented work on using current measurements to predict acoustic power (if the efficiency is known), however techniques proposed so far are not immune to harmonic distortion [47]. In this study we will augment this original work by testing both switched and linear amplifiers and observing the effects of two power measurement techniques on lesion formation.

III. Proposed Methodology

To measure active (dissipated) power, the time varying RMS voltage and current values are transformed into the frequency domain using an FFT and multiplied together:

$$S(f) = V(f) \times I(f)^* \tag{3}$$

The complex conjugate of $I(f)$ is used so that a leading current results in negative reactive power. The real component of $S(f)$ is integrated between two bounds:

$$P_{\text{total}} = \frac{\int_{f_0}^{f_1} Re\{S(f)\}df}{f_1 - f_0} \tag{4}$$

The values of f_0 and f_1 should be chosen to include any signal greater than -20 dB. Where 0 dB refers to the peak magnitude of $Re\{S(f)\}$. For example, with a 1.1 MHz SonicConcepts H-102 HIFU transducer that has been widely used in a number of pre-clinical studies, this equates to $f_0 =$ 0.5 MHz and $f_1 = 5$ MHz. The values of f_0 and f_1 are chosen so that the integration is significantly more broadband than the device's centre frequency. Making the bandwidth large improves the accuracy because harmonics generated by the drive circuit or device are included. The bounds must be limited however so as to reject cumulative high frequency noise. The -20 dB threshold was chosen heuristically to give accurate results. $I(t)$ can be obtained via a current probe, or current shunt and differential amplifier. The current along with $V(t)$ may be captured by a data acquisition Oscilloscope. An FFT should be used to transform the data into the frequency domain. P_{total} represents the total active power in Watts. The total acoustic power (also in Watts), W then is simply $\eta \times P_{\text{total}}$, where η is the efficiency of the transducer.

IV. Validation With Radiation Force Balance

The technique was first validated using a radiation force balance (Precision Acoustics Ltd, UK). Two common single element focused HIFU transducers (H102, Sonic Concepts, USA) and a *10-strip*, segmented array transducer (M102-065, Immasonic, France) were tested.

All transducers are manufactured from PZT. The 10-strip is 11 cm in diameter, with a 5 cm bore for an imaging array. It has a focus of 15 cm and is linearly segmented into 10 *strips* across the diameter of the transducer. More details on the manufacture of the 10-strip can be found in [48]. The diameter of the H102 transducers are 64 mm and their focal distance is 63 mm. At the time of the experiment, one of the H102 transducers was 6 months old and had been excited for less than 1 hour totally in its lifetime (H102-079). The older of the two was 6 years old and had been excited for approximately 6 hours totally in its lifetime (H102-065). The distinction is made so that the effects of degradation can be considered. They were otherwise identical.

All of the transducers were used with their manufacture-provided matching networks. The impedance of all three transducers were measured in water using a short cable and an impedance analyser (Bode 100, Omicron, USA). For the 10-strip, the matching network simply combines all the elements in parallel, so that the impedance was $50\,\Omega$, $\vartheta \approx 0$ at 1 MHz. The H102 transducers use a transformer based matching network, so that the impedance was $50\,\Omega$, $\vartheta \approx 0$ at 1.1 MHz. While the 10-strip is most effective at 1.0 MHz it has a broad bandwidth so is usually driven at 1.7 MHz to increase absorption in tissue [41]. At 1.7 MHz, the impedance was approximately $7\,\Omega$, $\vartheta = 17°$.

All of the HIFU transducers were driven by a typical linear amplifier (100A400AM6, AR RF/Microwave Instrumentation, USA). A signal generator (33250A, Keysight Technologies UK Ltd, Berkshire, UK) was connected to the input of the amplifier. A current probe (TM502A, Tektronix Inc., USA) was clamped around the positive input of the associated matching network to measure current flowing between the transducer and the amplifier. The probe amplifier was set to $50\,\mathrm{mA}$ per $10\,\mathrm{mV}$. The voltage across the matching network was simultaneously measured using an oscilloscope (WaveRunner, LeCroy, USA). Time delays due to cable lengths were calibrated out using a purely resistive 50 Ω load. A total of 1000 cycles from the oscilloscope were saved for the purposes of averaging. The oscilloscope sampling frequency was 200 MHz. The electrical connections used are shown in the grey box of figure 1.

For the radiation force balance (RFB), a 10 cm diameter calibrated absorber (Precision Acoustics Ltd, UK) was suspended in water from a set of high precision scales. Degassed, deionised water was used which was allowed to rest for 30 minutes so that the temperature was close to that of the room ($23\,°\mathrm{C}$). The transducer was mounted concentric to the absorber at a distance where it encompassed all of the acoustic energy but remained in the pre-focal region. This was approximately 2 cm for the H102s and 5 cm for the 10-strip. For each test, the off-on-off cycle of acoustic power was measured four times. Three measurements made up each off-on-off cycle: m_{off1} with the transducer de-energised, m_{on} 10 seconds into the transducer being energised and m_{off2} 10 seconds after the transducer had been de-energised. In accordance with the manufacturer's recommendations for making accurate measurements, the loss of water by evaporation above the target was compensated for by using the mean mass difference of each measurement. This was calculated as follows:

$$m = \frac{(m_{\mathrm{on}} - m_{\mathrm{off1}}) + (m_{\mathrm{on}} - m_{\mathrm{off2}})}{2} \tag{5}$$

m was then averaged over the 4 repeats and the following equation was used to calculate the power:

$$W = mcgF \tag{6}$$

W is the total acoustic power in Watts, c is the speed of sound, g is the gravitational constant and F is the calibration factor (0.95-1), which was established by a measurement standards laboratory (National Physical Laboratory, London, UK) and described the input/output power ratio of the target. $cgF \approx 14.5\ \mathrm{mW\,mg^{-1}}$.

The scales, signal generator and oscilloscope were all connected to a computer to automate the measurement. To test the scheme across a range of acoustic powers, the signal generator was programmed by a laptop computer to produce waveforms with a peak to peak voltage between $25\,\mathrm{mV}$ and $350\,\mathrm{mV}$ in intervals of $25\,\mathrm{mV}$. Given the geometry of the transducer and the gain of the amplifier, $350\,\mathrm{mV}$ corresponds approximately to a peak positive pressure of 8.72 MPa and a peak negative pressure of 7.00 MPa.

Active electrical power was measured in two ways (a) using voltage-only and the complex impedance ($Re\{V^2/Z\}$) and (b) by using the proposed technique. Measurement were performed simultaneously. The measured electrical powers were compared against the actual achieved acoustic powers for all three transducers.

Additionally, using only the H102-079 transducer, the robustness of the scheme to harmonic distortion in the drive waveform was tested. This was achieved by exciting the transducer using a square wave. The purpose of this was to simulate harmonic distortion brought about by a switched circuit (eg class D). This was done to ascertain whether the harmonic distortion influenced the reliability of voltage as a control.

V. Thermal Lesion Study

The CCV method can predict acoustic power irrespective of the relationship between source and load impedance. In this second study, the impact of this on lesion formation was assessed. To do this, the lesioning efficacy of a switched system was compared with a linear amplifier system. Lesions were made using the older of SonicConcepts transducer (H102-065) at electrical powers of 16 and 26 W. Using a reported efficiency of 70%, and an estimation of the beam width ($1.3\,\mathrm{mm}$) these should correspond approximately to spatial-average pulse-average intensities of 843 ± 148 and 1371 ± 238 $\mathrm{W\,cm^{-2}}$ respectively. A reduction in electrical power should reduce the lesion volume and if the power monitoring scheme

TABLE I
SYSTEM SETTINGS TO ACHIEVE DESIRED ACOUSTIC POWER USING VOLTAGE ONLY (*) AND COMBINED CURRENT AND VOLTAGE CALIBRATIONS

Power [W]	HIFUARP [%]	Signal gen. [mV]
16	68	195
16(*)	65	208
26	84	260
26(*)	85	240

is effective, the lesion volumes should be similar irrespective of the excitation circuit used for a given electrical power.

For the linear amplifier experiments, a signal generator (33600A, Agilent, USA) was connected to a 45 dB linear power amplifier (A150, E&I Ltd, USA) (figure 1). This amplifier was chosen over the one used in the previous study due to the continuous power ratings being higher. For the lesions made with a switched circuit, the High Intensity Focused Ultrasound Array Research Platform (HIFUARP) was used [25]. The switched system had voltage rails that were set to asymmetric values to compensate for the different resistances of the P and N channel MOSFETs, such that the maximum and minimum possible voltage values were ± 68 V. The 5-level HRPWM modulation algorithm was used to design the switched waveforms [49]. The current and voltage at the input of the matching network was monitored as described in the previous section.

Each system was calibrated to produce the same acoustic intensity in two ways. The first set of lesions were formed when both systems were calibrated using the active power calculated using voltage-only and impedance. The second set of lesions were formed when both systems were calibrated using CCV (the proposed technique). For each calibration technique, at both powers, three lesions were made, leading to a total of 24 lesions. The results of each calibration are shown in table I. The HIFUARP system uses PWM to drive the transducer, so it's values represent pulse-width. At 100% the waveform is a perfect square wave, but at lower percentages the waveform uses additional levels to better approximate a sine wave. Hence as the amplitude changes the relative distortion of the waveform also changes. The table shows that since harmonic distortion cannot be guaranteed across amplitudes, pulse width does not scale linearly with acoustic power. The signal generator column represents the magnitude of the input stage to the linear amplifier.

Ex vivo chicken breast was used as a tissue mimic for the lesioning study. Fresh tissue was exposed to ultrasound within 18 hours of purchase and was refrigerated at $4\,^{\circ}\mathrm{C}$ when not used. The samples were cut into cubes approximately $55\ \mathrm{mm} \times 55\ \mathrm{mm} \times 40\ \mathrm{mm}$. The samples were then degassed in a 1% (v/v) phosphate buffer solution for 4 hours. To ensure repeatability between samples, they were placed in a holder marginally smaller than their cut size so that they were slightly compressed in all directions. The sample holder had acoustic windows on opposite sides of approximately $50\ \mathrm{mm} \times 50\ \mathrm{mm}$ (figure 1).

The sample holder was attached to a CNC machine stage. To co-locate the centres of the transducer focus and the samples, an alignment target was temporarily attached to the inside of the sample holder, prior to the start of the first exposure. Using a hydrophone (Y-107, Sonic Concepts, USA) co-located and confocal with the centre of the HIFU transducer, the transducer focus was pulse-echo positioned onto the target. The CNC stage was programmed to move to 5 fixed locations spaced $20\,\mathrm{mm}$ apart. This meant that the 5 lesions were always made in the same locations and at a fixed depth of $20\,\mathrm{mm}$ in each sample. Sonications were performed in a tank of degassed, deionised water which was maintained at $28 \pm 1\ ^{\circ}\mathrm{C}$ using an immersion circulator. Although lower than the normothermia temperature of 37° C, this temperature was chosen to be representative of *in vivo* tissue without causing premature denaturing of the sample.

To attenuate post-focal energy and prevent reflections, $10\,\mathrm{mm}$ of absorbing material was placed behind the samples. The opening of the sample holder was significantly larger than the focus and the transducer was placed in the centre of the tank to reduce the risk of reflections influencing acoustic propagation. The samples were sonicated for $20\,\mathrm{s}$, and between exposures, the tissue was allowed to cool for $10\,\mathrm{s}$. The experiment schematic is depicted in figure 1.

Immediately after all the exposures were complete, samples were sliced through the centre of the lesions, revealing two halves of each lesion. Photographs of each lesion were taken next to a ruler and an identifying code. Using image analysis software (ImageJ, National Institutes for Health, USA), the pixel/size ratio was calculated and then the lesion cross section area was measured using an ellipse area tool. Lesions cross section areas were then compared.

For the lesioning efficacy of different calibration schemes to be compared we aimed to ensure that damage to the tissue was predominantly thermal in nature and not from mechanical effects such as acoustic cavitation and/or boiling [50]. Three measures were taken to ensure that mechanical damage was reduced. Firstly, a threshold-based passive cavitation detector (PCD) system was used [25], [50]. Secondly, exposure times and intensities within the limits of previously published lesioning work (in chicken breast) were used [51]. Thirdly, lesions were inspected for unusual shapes that may suggest boiling.

To ensure that each tissue sample was adequately degassed, prior to lesion formation, a high amplitude ($p \approx 2$ MPa) 5 cycle pulse was applied to the transducer to discount the presence of bubbles. It was expected that the presence of bubbles would have a harmonic response and therefore trigger the PCD. Lesions where cavitation activity occurred were discarded and not included in further analysis.

VI. RESULTS

Figure 2 shows the difference between measured acoustic power (from RFB) and predicted power (electrical power $\times$ efficiency) for each transducer. When the difference is zero, the predicted acoustic power (electrical power $\times$ efficiency) matches actual acoustic power perfectly. When the error is positive the predicted power is higher than the acoustic power and vice versa. The blue lines represent the H102-079 transducer

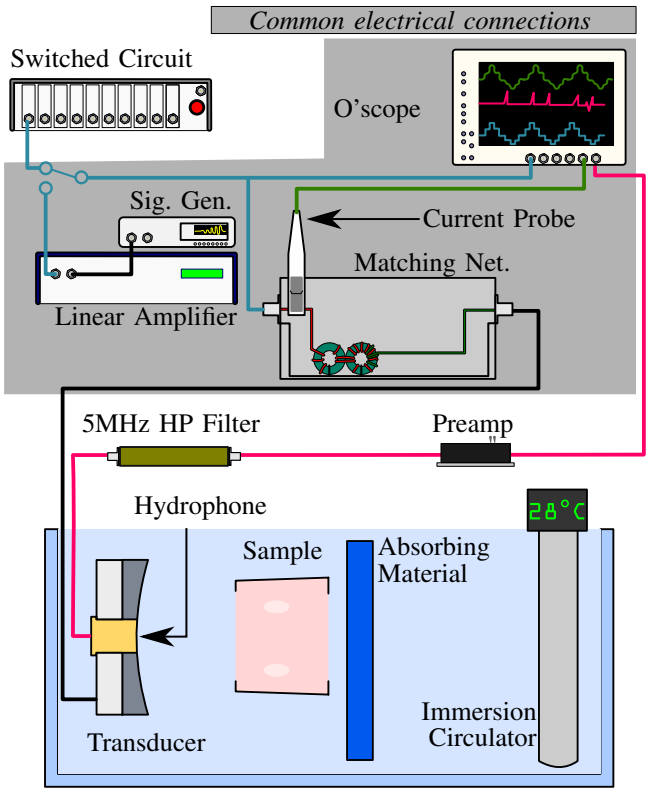

Fig. 1. Schematic of the experimental apparatus used in this study. Not shown: CNC machine. The grey box highlights the electrical connections that were common between the validation and lesioning experiments.

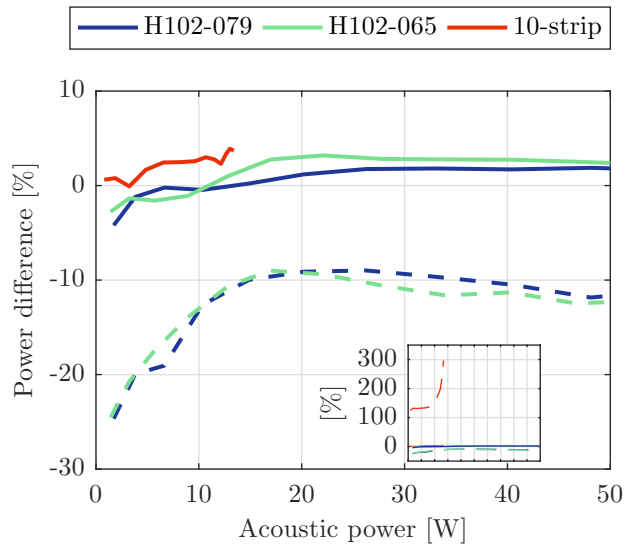

Fig. 2. Difference between the acoustic power (obtained from a RFB) and electrical power (once efficiency is accounted for). The electrical power was measured using CCV (the proposed technique, solid line) and using voltage only (dashed line). Three transducers were considered, a new H102 transducer (blue line), an old H102 transducer (green line) and a 10-strip transducer (red line). Only the first 50 Watts are shown. Inset: Same data zoomed out, to a larger axis which makes the 10-strip's data visible. Not shown: Measurement error corresponds to about ±6%.

while the H102-065 is represented by the green lines. The 10-strip is represented by the red lines. Here and in figure 3, the dashed lines represent power predictions using VO, while CCV (the proposed technique) is represented by the solid lines. Inset is the same data but on a large y axis, to make the 10-strip VO-measured power data visible. Figure 3 shows the difference for both electrical excitations. The power obtained using the sine waves and square waves are represented by the blue and red lines respectively. For both figures, values for efficiency (η) were obtained using values from the transducer datasheets (75% for the H102s and 85% for the 10-strip). The actual exact value of efficiency is not critical since the aim of the measurement technique is to be as reliable as possible, ie, produce the least variation in power across a range of acoustic powers.

Figure 4 shows the lesion cross-sectional areas obtained when using voltage-only (*) and CCV (the proposed technique) to calibrate the electrical powers. The lesions formed by the linear amplifier are represented by the blue bar, while the switched circuit system's lesions are represented by green bars. The red bars show the absolute difference in mean lesion size between the systems. The error bars represent the standard deviation of the three measurements, where each measurement corresponds to a new lesion formed and measured by the same operator.

Statistical tests were undertaken on the data. Firstly, each set of repeats were tested for normality using the Shapiro-Wilk test which is ideal for small sample sizes [52]. All sets

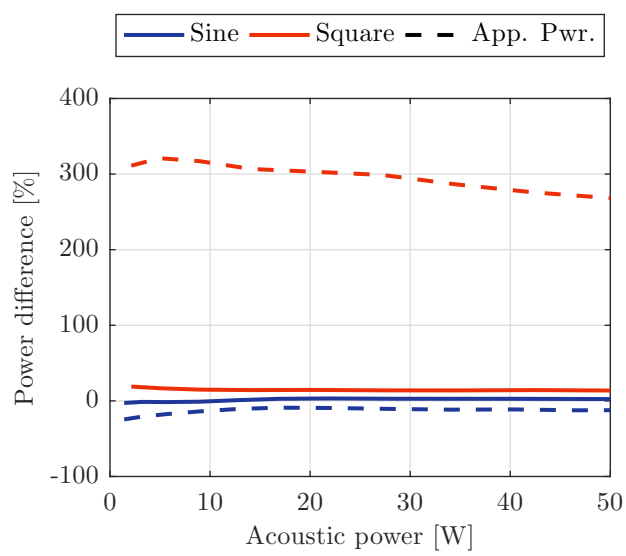

Fig. 3. Difference between the acoustic power (obtained from a RFB) and electrical power (once efficiency is accounted for). Two different excitation schemes were tested, square wave (red) and a sinusoidal wave (blue). The solid lines represent CCV-measured power, and the dashed lines represent VO-measured power. Tested with H102-079 only. Not shown: Measurement error corresponds to about ±6%.

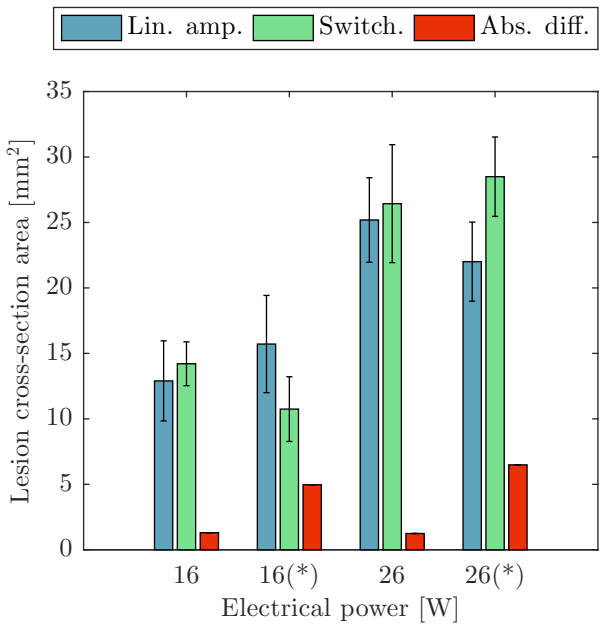

Fig. 4. Thermal lesion cross-section areas obtained in using a linear amplifier and using a switched circuit. Lesions were made using electrical powers of 16 W and 26 W. Lesions formed when the circuits were calibrated using power calculated from impedance and voltage are indicated by *. In the other instances, the circuits were calibrated using current and voltage (CCV) measurements. The red bars represent the absolute difference between the lesion sizes.

TABLE II
RESULTS OF STATISTICAL TESTS PERFORMED ON LESION DATA

Power [W]	p_{av}	$\sigma_{\mathrm{sw}} - \sigma_{\mathrm{lin}}$
16	0.55	+10%
16(*)	0.13	-38%
26	0.72	+4.9%
26(*)	0.06	+25%

of repeats did not reject the null hypothesis ($p_{\mathrm{sw}} > 0.05$) except for the lesions produced using the linear amplifier at 16(*) W ($p_{\mathrm{sw}} < 0.05$). Analysis of variance (ANOVA) was then performed on the data. Despite the normality test rejecting the null hypothesis on some of the data, the analysis was still undertaken as ANOVA has high immunity to non-normality and the probability of non-normality was close to the threshold.

ANOVA was performed to assess similarity between schemes at the same power and calibration technique (p_{av}). The results of the statistical tests made on the lesion data are given in table II.

VII. Discussion

With the efficiency of the transducers taken into consideration, the difference between the predicted acoustic power and actual acoustic power varied between -20% and -9% when the proposed scheme was not used (fig. 2). Conversely when the proposed scheme was used the variation was between only -5% and +3%. For the 10-strip transducer, again using only voltage, the difference began at 128% and increased rapidly to a maximum of 304% which can likely be attributed to reflections from transmission line effects. Using the proposed scheme, the difference was between only 1% and 4% over the same range of acoustic power.

Good matching of the H102 transducers and amplifier were verified using a impedance analyser (Bode 100, Omicron, USA). Despite this, the results show there was a large difference power measured using VO and CCV. The power error varies considerably with acoustic power and cannot be accounted for by adjusting the efficiency value, η.

For each measurement point, standard deviation of difference was calculated from the 4 repeat measurements made with the RFB. Error from the electrical measurements was not considered as it was several orders of magnitude smaller than the error from the RFB. The standard deviation showed that the variation in radiation force balance measurements contributed less than $\pm 6\%$ error and typically less than 2%.

If the acoustic power is known, it is possible to predict the pulse-average spatial-average intensity (I_{SAPA}) by dividing the total electrical power by the flux area of the beam. With the H102 transducers, 40 W corresponds to an approximate intensity of 3013 $\mathrm{W\,cm^{-2}}$, meaning VO-measured power measurement equates to a prediction error of +301 $\mathrm{W\,cm^{-2}}$. At the same acoustic power, substituting with CCV-measured power could reduce this to -60 $\mathrm{W\,cm^{-2}}$. For the 10-strip, 13 W corresponds to an intensity of 1207 $\mathrm{W\,cm^{-2}}$ which equates to an error of -3669 $\mathrm{W\,cm^{-2}}$ when VO is used. Again, this could be reduced to +44$\mathrm{W\,cm^{-2}}$ using CCV-measured power. Above 20 W, acoustic streaming effects may contribute to some of the error but this is expected to be minor compared to experimental error. Despite the amplifier being a class-A type, the variation in the VO-power is attributed to distortion in the amplifier output and a variance in transducer acceptance with voltage.

When square wave excitation was used (fig. 3) the VO-measured power difference was also considerable (nominally +300%). However, unlike the experiment which instead compared transducers, the contributing factor here was the large amount of reactive power at each of the harmonics in the square wave.

The results show that CCV-measured power can compensate for both harmonic distortion, reactance and reflections. However, the usefulness of the technique as a predictor of intensity does rely on η being constant, when in fact it is known to change with both frequency and voltage. In terms of frequency variance, equation 4 was made broadband to include drive waveform distortion or harmonics generated by the transducer. Since the real components will likely be smaller than the central drive frequency, the impact of not properly weighting η should be minor. Although predicting acoustic power in the presence of drive-waveform distortion is already greatly improved using the proposed technique, drive circuitry distortion could be factored into the efficiency calculation to improve the accuracy of the technique. The proposed method controls effective electric power and there are some circumstances this may sometimes not be exactly relating to acoustic power, in particular, if the transducer efficiency is affected. One limitation of the proposed technique

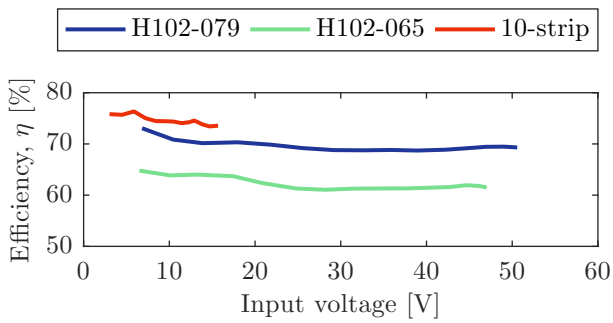

Fig. 5. The efficiency of the three HIFU transducers as a function of input voltage. H102-079 is approximately 6 months old and has seen very little use. H102-065 has been used regularly over the past 6 years. In accordance with the manufacture directions for the linear amplifier, 10-strip testing above 16 V was not conducted to protect the amplifier from reflected energy due to the low impedance of the transducer.

is that it may not be possible to detect these issues if the efficiency were to be affected. However, it is possible that in an integrated system a lower effective electric power would be obtained for the same driving voltage and this would indicate damage, this should be explored in future work.

Efficiency variance with voltage was measured across a range of peak voltages for all three transducers. For this test, voltage was measured at the output of the linear amplifier and the electrical power was measured using the proposed technique. The linear amplifier (driven by a function generator) was used to minimise harmonic distortion in the drive waveform. The results are shown in figure 5. It can be seen that the older of the H102 transducers (H102-065) is approximately 10% less efficient than the newer one. Overall, η varied less than 5% so will not have a big impact on the results.

The lesioning results (fig. 4) show that lesion volume increases as the electrical power is increased. The lesions have a nominal cross-sectional area of 14 mm^2 at 16 W and 26 mm^2 at 26 W.

When CCV was used to calibrate the circuits and subsequently perform lesioning, there was better agreement between the lesion sizes. This can be quantified as follows: At 16 W the lesions formed by the switched circuit had a mean 1.3 mm^2 (10%) larger than when the the linear amplifier was used. At 26 W, the lesions had a mean 1.2 mm^2 (5%) larger. However, when VO-measured power was used to calibrate the circuits, there was poor agreement between the lesion sizes: At 16(*) W, the lesions formed using the switched circuit had a mean 5.0 mm^2 smaller (38%) and at 26(*) W the mean was 6.5 mm^2 (25%) larger.

As expected, there was an increase in lesion size as the magnitude of the excitation parameters increased. Although attempts were made to minimise the difference in power between the switched and linear amplifier system using both power measurement techniques, the relationship between the two calibration schemes was not consistent across power levels. Referring to I, with the switched system between 16(*) W and 16 W there was a +3% difference in the calibration result. However for the same system there was a -1% change between 26(*) W and 26 W. This inconsistency can be attributed to higher-order harmonic content of the HRPWM waveforms which is known to change with amplitude, and cannot be compensated for without using the proposed technique. The effect of this was that the difference between the switched circuit and linear amplifier mean lesion size was negative at 16(*) W but was positive at 26(*) W.

The ANOVA results (table II) show that there is no statistically significant difference between the lesion sizes. However, since the sample size is fixed, the p_{av} values can be compared which shows there is better agreement in the lesion size when CCV was used at 16 W ($0.55 > 0.13$) and at 26 W ($0.72 \gg 0.06$). Only the minimum number of repeats required to perform ANOVA analysis were performed, which reduces the statistical power of the test. However, given that the effects were observed at two different power levels, the probability that type II error influenced the conclusion was low.

In the study, measurements were not made on the transducer side of the matching network. It may have been more accurate to instead measure the transducer side. However, since the impedance was measured with the matching network in place and the load attached, the only source of error should be from insignificant heating losses in the network. The proposed technique should work either side of the network. This is important given that the matching network may or may not be located near the driving electronics. At 10 W of acoustic power using the H102-065, no discernable difference was observed between post and pre-network measurements. Where matching networks are not used, the clamp on current probe could be replaced with a very low-loss MRI-compatible PCB Regowski coil, or differential amplifier. Commercial systems may already be implementing current monitoring on the power supply rails of array systems, but this is not evident from current literature and cannot discern differences in the properties of individual elements in the array.

Just as with a RFB, predicting the resulting acoustic power in the presence of bone or cavitation is complex. In transcranial ultrasound, low frequencies ($<$ 1 MHz) are used and the skull encompasses all of the transducer field so acoustic scattering is fairly uniform and predictable. The proposed scheme will be most suited to transcranial applications. For transcostal applications, the interleaved nature of the rib cage means that treatment planning remains a challenge. The proposed technique may be useful in detecting cavitation however as transducer impedance is known to change during cavitation events [41].

Through the experiments with square wave excitation and switched circuit lesioning, it has been shown that the technique is highly immune to harmonic distortion. This is because there is access to both voltage and current waveforms, so the technique inherently compensates or the direction of flow at all frequencies. Thus, the technique could be useful for class-D HIFU systems and histrotripsy sources [53]. However, since the latter is not a predominately thermal technique, acoustic power may be less useful than peak positive pressure is. The technique could be useful in the real time monitoring of lesion formation.

Overall, the results show that VO-measured power can not reliably be used to predict acoustic power and that the errors

are sufficiently large enough to influence lesion size. These errors are greatly reduced when using CCV-measured power which produces lesions of consistent size.

VIII. Conclusions

Electrical power during HIFU therapy must be monitored to avoid either under or overexposure and ensure patient safety. In this paper it was shown that voltage monitoring alone is not sufficient to monitor acoustic power. Instead combined voltage and current monitoring, which could be integrated into drive circuity, was combined to measure dissipated power.

The results showed that this technique can accurately predict acoustic power. The use of current monitoring will facilitate improvements in safety and practicality of HIFU systems, by ensuring that acoustic power can be reliably controlled.

Acknowledgements

The authors would like to thank Gail Ter Haar and Ian Rivens for loan of the 10-strip HIFU transducer. The authors would also like to acknowledge the ThUNDDAR network for its continued support.

References

[1] G. Ter Haar, "Ultrasound focal beam surgery," *Ultrasound in medicine & biology*, vol. 21, no. 9, pp. 1089–1100, 1995.

[2] M. Lee, D. Schlesinger, G. ter Haar, B. Sela, M. Eames, J. Snell, A. Hananel, N. Kassell, J. Sheehan, J. Larner *et al.*, "Thermal dose and radiation dose comparison based on cell survival," *Journal of Therapeutic Ultrasound*, vol. 3, no. 1, p. P26, 2015.

[3] J. R. McLaughlan, D. M. Cowell, and S. Freear, "Gold nanoparticle nucleated cavitation for enhanced high intensity focused ultrasound therapy," *Physics in medicine and biology*, 2017.

[4] D. McMahon, C. Poon, and K. Hynynen, "Increasing bbb permeability via focused ultrasound: Current methods in preclinical research," *Blood-Brain Barrier*, vol. 26, p. 267, 2019.

[5] Z. Xu, A. Ludomirsky, L. Y. Eun, T. L. Hall, B. C. Tran, J. B. Fowlkes, and C. A. Cain, "Controlled ultrasound tissue erosion," *IEEE transactions on ultrasonics, ferroelectrics, and frequency control*, vol. 51, no. 6, pp. 726–736, 2004.

[6] Z. Izadifar, P. Babyn, and D. Chapman, "Mechanical and biological effects of ultrasound: A review of present knowledge," *Ultrasound in Medicine & Biology*, 2017.

[7] V. A. Khokhlova, M. R. Bailey, J. A. Reed, B. W. Cunitz, P. J. Kaczkowski, and L. A. Crum, "Effects of nonlinear propagation, cavitation, and boiling in lesion formation by high intensity focused ultrasound in a gel phantom," *The Journal of the Acoustical Society of America*, vol. 119, no. 3, pp. 1834–1848, 2006.

[8] C. J. Diederich, "Thermal ablation and high-temperature thermal therapy: overview of technology and clinical implementation," *International journal of hyperthermia*, vol. 21, no. 8, pp. 745–753, 2005.

[9] L. Zhang and Z.-B. Wang, "High-intensity focused ultrasound tumor ablation: review of ten years of clinical experience," *Frontiers of medicine in China*, vol. 4, no. 3, pp. 294–302, 2010.

[10] J. E. Kennedy, "High-intensity focused ultrasound in the treatment of solid tumours," *Nature reviews cancer*, vol. 5, no. 4, pp. 321–327, 2005.

[11] R. Illing, J. Kennedy, F. Wu, G. Ter Haar, A. Protheroe, P. Friend, F. Gleeson, D. Cranston, R. Phillips, and M. Middleton, "The safety and feasibility of extracorporeal high-intensity focused ultrasound (HIFU) for the treatment of liver and kidney tumours in a western population," *British journal of cancer*, vol. 93, no. 8, p. 890, 2005.

[12] A. Blana, F. J. Murat, B. Walter, S. Thuroff, W. F. Wieland, C. Chaussy, and A. Gelet, "First analysis of the long-term results with transrectal HIFU in patients with localised prostate cancer," *european urology*, vol. 53, no. 6, pp. 1194–1203, 2008.

[13] N. Sanghvi, F. J. Fry, R. Bihrle, R. Foster, M. Phillips, J. Syrus, A. Zaitsev, and C. Hennige, "Noninvasive surgery of prostate tissue by high-intensity focused ultrasound," *IEEE Transactions on Ultrasonics, Ferroelectrics, and Frequency Control*, vol. 43, no. 6, pp. 1099–1110, 1996.

[14] M. Peek, M. Ahmed, A. Napoli, B. ten Haken, S. McWilliams, S. Usiskin, S. Pinder, M. Van Hemelrijck, and M. Douek, "Systematic review of high-intensity focused ultrasound ablation in the treatment of breast cancer," *British journal of surgery*, vol. 102, no. 8, pp. 873–882, 2015.

[15] D. Coluccia, J. Fandino, L. Schwyzer, R. O'Gorman, L. Remonda, J. Anon, E. Martin, and B. Werner, "First noninvasive thermal ablation of a brain tumor with MR-guided focusedultrasound," *Journal of therapeutic ultrasound*, vol. 2, no. 1, p. 17, 2014.

[16] K. Hynynen, G. T. Clement, N. McDannold, N. Vykhodtseva, R. King, P. J. White, S. Vitek, and F. A. Jolesz, "500-element ultrasound phased array system for noninvasive focal surgery of the brain: a preliminary rabbit study with ex vivo human skulls," *Magnetic resonance in medicine*, vol. 52, no. 1, pp. 100–107, 2004.

[17] G. Maimbourg, A. Houdouin, T. Deffieux, M. Tanter, and J.-F. Aubry, "3D-printed adaptive acoustic lens as a disruptive technology for transcranial ultrasound therapy using single-element transducers," *Physics in Medicine and Biology*, 2017.

[18] C. Adams, J. McLaughlan, L. Nie, and S. Freear, "Excitation and acquisition of cranial guided waves using a concave array transducer," in *Proceedings of Meetings on Acoustics 173EAA*, vol. 30, no. 1. ASA, 2017, p. 055003.

[19] C. Adams, D. M. Cowell, L. Nie, J. R. McLaughlan, and S. Freear, "A miniature HIFU excitation scheme to eliminate switching-induced grating lobes and nullify hard tissue attenuation," in *Ultrasonics Symposium (IUS), 2017 IEEE International*. IEEE, 2017, pp. 1–4.

[20] H. E. Cline, J. Schenek, K. Hynynen, and R. D. Watkins, "MR-guided focused ultrasound surgery," *Journal of computer assisted tomography*, vol. 16, pp. 956–956, 1992.

[21] J. Kennedy, G. Ter Haar, and D. Cranston, "High intensity focused ultrasound: surgery of the future?" *The British journal of radiology*, vol. 76, no. 909, pp. 590–599, 2003.

[22] E. Boni, C. Alfred, S. Freear, J. A. Jensen, and P. Tortoli, "Ultrasound open platforms for next-generation imaging technique development," *IEEE Transactions on Ultrasonics, Ferroelectrics, and Frequency Control*, 2018.

[23] G. Fleury, R. Berriet, J. Y. Chapelon, G. ter Haar, C. Lafon, O. Le Baron, L. Chupin, F. Pichonnat, and J. Lenormand, "Safety issues for HIFU transducer design," in *AIP Conference Proceedings*, vol. 754, no. 1. AIP, 2005, pp. 233–241.

[24] M. M. El-Desouki and K. Hynynen, "Driving circuitry for focused ultrasound noninvasive surgery and drug delivery applications," *Sensors*, vol. 11, no. 1, pp. 539–556, 2011.

[25] C. Adams, T. M. Carpenter, D. Cowell, S. Freear, and J. R. McLaughlan, "HIFU drive system miniaturization using harmonic reduced pulsewidth modulation," *IEEE transactions on ultrasonics, ferroelectrics, and frequency control*, vol. 65, no. 12, pp. 2407–2417, 2018.

[26] W. Wong, C. Christoffersen, S. Pichardo, and L. Curiel, "An integrated ultrasound transducer driver for HIFU applications," in *Electrical and Computer Engineering (CCECE), 2013 26th Annual IEEE Canadian Conference on*. IEEE, 2013, pp. 1–5.

[27] C. Christoffersen, W. Wong, S. Pichardo, G. Togtema, and L. Curiel, "Class-de ultrasound transducer driver for HIFU therapy," *IEEE transactions on biomedical circuits and systems*, vol. 10, no. 2, pp. 375–382, 2016.

[28] N. Lipsman, M. L. Schwartz, Y. Huang, L. Lee, T. Sankar, M. Chapman, K. Hynynen, and A. M. Lozano, "Mr-guided focused ultrasound thalamotomy for essential tremor: a proof-of-concept study," *The Lancet Neurology*, vol. 12, no. 5, pp. 462–468, 2013.

[29] J. Song and K. Hynynen, "Feasibility of using lateral mode coupling method for a large scale ultrasound phased array for noninvasive transcranial therapy," *IEEE Transactions on Biomedical Engineering*, vol. 57, no. 1, pp. 124–133, 2009.

[30] K. Hynynen and R. M. Jones, "Image-guided ultrasound phased arrays are a disruptive technology for non-invasive therapy," *Physics in Medicine & Biology*, vol. 61, no. 17, p. R206, 2016.

[31] A. D. Maxwell, G. Owens, H. S. Gurm, K. Ives, D. D. Myers Jr, and Z. Xu, "Noninvasive treatment of deep venous thrombosis using pulsed ultrasound cavitation therapy (histotripsy) in a porcine model," *Journal of vascular and interventional radiology*, vol. 22, no. 3, pp. 369–377, 2011.

[32] I. E. Commission *et al.*, "Ultrasonics—field characterization—specification and measurement of field parameters for high intensity therapeutic ultrasound (HITU) transducers and systems," 2014.

[33] Y. Zhou, L. Zhai, R. Simmons, and P. Zhong, "Measurement of high intensity focused ultrasound fields by a fiber optic probe hydrophone,"

The Journal of the Acoustical Society of America, vol. 120, no. 2, pp. 676–685, 2006.

[34] M. S. Canney, M. R. Bailey, L. A. Crum, V. A. Khokhlova, and O. A. Sapozhnikov, "Acoustic characterization of high intensity focused ultrasound fields: A combined measurement and modeling approach," *The Journal of the Acoustical Society of America*, vol. 124, no. 4, pp. 2406–2420, 2008.

[35] A. Ramos, J. L. San Emeterio, and P. T. Sanz, "Improvement in transient piezoelectric responses of NDE transceivers using selective damping and tuning networks," *IEEE transactions on ultrasonics, ferroelectrics, and frequency control*, vol. 47, no. 4, pp. 826–835, 2000.

[36] R. Thurston, "Effect of electrical and mechanical terminating resistances on loss and bandwidth according to the conventional equivalent circuit of a piezoelectric transducer," *IRE*.

[37] J. Song, B. Lucht, and K. Hynynen, "Large improvement of the electrical impedance of imaging and high-intensity focused ultrasound (hifu) phased arrays using multilayer piezoelectric ceramics coupled in lateral mode," *IEEE transactions on ultrasonics, ferroelectrics, and frequency control*, vol. 59, no. 7, pp. 1584–1595, 2012.

[38] E. Hutchinson, M. Buchanan, and K. Hynynen, "Design and optimization of an aperiodic ultrasound phased array for intracavitary prostate thermal therapies," *Medical physics*, vol. 23, no. 5, pp. 767–776, 1996.

[39] Y. Zhou, "Acoustic power measurement of high-intensity focused ultrasound transducer using a pressure sensor," *Medical engineering & physics*, vol. 37, no. 3, pp. 335–340, 2015.

[40] R. Ramesh and D. Ebenezer, "Equivalent circuit for broadband underwater transducers," *IEEE transactions on ultrasonics, ferroelectrics, and frequency control*, vol. 55, no. 9, pp. 2079–2083, 2008.

[41] J. R. McLaughlan, "An investigation into the use of cavitation for the optimisation of high intensity focused ultrasound (HIFU) treatments," Ph.D. dissertation, University of London, Sep. 2008. [Online]. Available: https://doi.org/10.5281/zenodo.1311683

[42] D. R. Daum, M. T. Buchanan, T. Fjield, and K. Hynynen, "Design and evaluation of a feedback based phased array system for ultrasound surgery," *ieee transactions on ultrasonics, ferroelectrics, and frequency control*, vol. 45, no. 2, pp. 431–438, 1998.

[43] J. Haller, K. Jenderka, A. Shaw, G. Durando, and B. Karaböce, "Metrology of high-intensity therapeutic ultrasound within the EMRP project 'external beam cancer therapy'. characterization of sources," *Metrologia*, vol. 49, no. 5, p. S267, 2012.

[44] M. T. Buchanan and K. Hynynen, "Design and experimental evaluation of an intracavitary ultrasound phased array system for hyperthermia," *IEEE transactions on biomedical engineering*, vol. 41, no. 12, pp. 1178–1187, 1994.

[45] D. R. Daum, N. B. Smith, R. King, and K. Hynynen, "In vivo demonstration of noninvasive thermal surgery of the liver and kidney using an ultrasonic phased array," *Ultrasound in medicine & biology*, vol. 25, no. 7, pp. 1087–1098, 1999.

[46] H. Faugel, V. Bobkov, H. Fünfgelder, G. Siegl, I. Stepanov, and A. U. Team, "Measuring impedance and power in ICRF antenna feeding lines with voltage and current probes," in *AIP Conference Proceedings*, vol. 1406, no. 1. AIP, 2011, pp. 113–116.

[47] B. Karaböce, Y. Gülmez, S. Rajagapol, and A. Shaw, "Instantaneous input electrical power measurements of HITU transducer," in *Journal of Physics: Conference Series*, vol. 279, no. 1. IOP Publishing, 2011, p. 012011.

[48] J. Civale, R. Clarke, I. Rivens, and G. Ter Haar, "The use of a segmented transducer for rib sparing in HIFU treatments," *Ultrasound in medicine & biology*, vol. 32, no. 11, pp. 1753–1761, 2006.

[49] D. Cowell, T. Carpenter, P. Smith, C. Adams, S. Harput, and S. Freear, "Performance of switched mode arbitrary excitation using harmonic reduction pulse width modulation (HRPWM) in array imaging applications," in *Ultrasonics Symposium (IUS), 2016 IEEE International*. IEEE, 2016, pp. 1–4.

[50] J. McLaughlan, I. Rivens, T. Leighton, and G. Ter Haar, "A study of bubble activity generated in ex vivo tissue by high intensity focused ultrasound," *Ultrasound in medicine & biology*, vol. 36, no. 8, pp. 1327–1344, 2010.

[51] P. Lai, J. R. McLaughlan, A. B. Draudt, T. W. Murray, R. O. Cleveland, and R. A. Roy, "Real-time monitoring of high-intensity focused ultrasound lesion formation using acousto-optic sensing," *Ultrasound in medicine & biology*, vol. 37, no. 2, pp. 239–252, 2011.

[52] W. W. Elliott AC, *Statistical analysis quick reference guidebook with SPSS examples*. Sage Publications, 2007.

[53] A. D. Maxwell, P. V. Yuldashev, W. Kreider, T. D. Khokhlova, G. R. Schade, T. L. Hall, O. A. Sapozhnikov, M. R. Bailey, and V. A. Khokhlova, "A prototype therapy system for transcutaneous application of boiling histotripsy," *IEEE transactions on ultrasonics, ferroelectrics, and frequency control*, vol. 64, no. 10, pp. 1542–1557, 2017.

Chris Adams (IEEE S'11-M'19) worked in industry for 2 years as an FPGA firmware designer following his undergraduate degree in electronic engineering. In 2019, he obtained his Ph.D. at the University of Leeds in the ultrasound group and subsequently worked as an Experimental Officer. He is now a postdoctoral fellow at the Sunnybrook Research Institute in Canada. His research interests include the application of electronics, systems, signal processing and algorithms to HIFU and NDT.

James R. McLaughlan Dr James McLaughlan is a medical physicist who undertook a PhD at the Institute of Cancer Research, investigating the optimisation of therapeutic ultrasound for cancer therapy using cavitation. He became a postdoctoral research fellow at Boston University, where he studied light absorbing nanoparticles for photoacoustic imaging. He moved to the University of Leeds in 2010 to work on next generation therapeutic microbubbles. In 2013 he was awarded a Leverhulme early career research fellowship to develop molecular-targeted gold nanoparticles for the detection and treatment of cancerous cells within breast tissue. Currently, he holds a joint academic position between the faculties of Engineering and Medicine and Health where his main research areas are non-invasive cancer therapies, molecular-targeted theranostics and semi-autonomous surgical systems.

Thomas M. Carpenter received the M.Eng. degree in electronic and electrical engineering from the University of Leeds, Leeds, U.K., in 2014. He joined the Georgia Institute of Technology, Atlanta, GA, USA, as a Research Engineer developing high-speed field-programmable gate array (FPGA) designs for ultrasound imaging applications. He is currently a Visiting Researcher with the Ultrasound Research Group, University of Leeds. His current research interests include embedded systems and FPGA design, both in the biomedical field and for industrial applications.

Steven Freear (IEEE S'95–M'97–SM'11) gained his doctorate in 1997 and subsequently worked in the electronics industry for 7 years as a medical ultrasonic system designer. He was appointed Lecturer (Assistant Professor), Senior Lecturer (Associate Professor) and then Professor in 2006, 2008 and 2016 respectively, at the School of Electronic and Electrical Engineering at the University of Leeds. In 2006, he formed the Ultrasound Group, specializing in both industrial and biomedical research. His main research interest is concerned with advanced analog and digital signal processing and instrumentation for ultrasonic systems. He teaches digital signal processing, VLSI and embedded systems design, and hardware description languages at both undergraduate and postgraduate levels. He was elected Editor-in-Chief in 2013 for the IEEE Transactions on Ultrasonics, Ferrorelectrics and Frequency Control. In June 2014 he was appointed Visiting Professor at Georgia Tech. He is External Examiner to undergraduate programmes in Electronic Engineering at Queen's University, Belfast.